$\overline{\mathsf{F}}_{1j} = \widehat{\mathsf{F}}_{1j} \cup \underline{s}_{1j}\widehat{\mathsf{F}}_{1j}$, the trivial layer group $\widehat{\mathsf{J}}_{1j} = \widehat{\mathsf{F}}_{1j} \cup r^*_{1j}\widehat{\mathsf{F}}_{1j}$ and the trivial layer group $\widehat{\mathsf{F}}_{1j}$.

An example of a symmetric reversible (SR) twin (and wall) is the twin $(\mathbf{S}_1[010]\mathbf{S}_2)$ in Fig. 3.4.4.2 with a non-trivial twinning operation $\underline{2}^\star_z$ and with reversing operations $\underline{m}_y$ and $m^\star_x$. The twin $(\mathbf{S}_1^+[\bar{1}10]\mathbf{S}_3^-)$ and reversed twin $(\mathbf{S}_3^-[\bar{1}10]\mathbf{S}_1^+)$ in Fig. 3.4.3.8 are symmetric and irreversible (SI) twins with a twinning operation $\underline{m}^\star_{xy}$; no reversing operations exist (walls are charged and charged walls are always irreversible, since a charge is invariant with respect to any transformation of the space). The twin $(\mathbf{S}_1^-[110]\mathbf{S}_3^+)$ and reversed twin $(\mathbf{S}_3^+[110]\mathbf{S}_1^-)$ in the same figure are asymmetric state-reversible twins with state-reversing operation $m^\star_{xy}$ and with no non-trivial twinning operation.

The same classification also applies to domain twins and walls in a microscopic description.

As in the preceding section, we shall now present separately the symmetries of non-ferroelastic simple domain twins ['twinning without a change of crystal shape (or form)'] and of ferroelastic simple domain twins ['twinning with a change of crystal shape (or form)'; Klassen-Neklyudova (1964), Indenbom (1982)].

3.4.4.4. *Non-ferroelastic domain twins and domain walls*

Compatibility conditions impose no restriction on the orientation of non-ferroelastic domain walls. Any of the non-ferroelastic domain pairs listed in Table 3.4.3.4 can be sectioned on any crystallographic plane p and the sectional group $\overline{\mathsf{J}}_{1j}$ specifies the symmetry properties of the corresponding twin and domain wall. The analysis can be confined to one representative orientation of each class of equivalent planes, but a listing of all possible cases is too voluminous for the present article. We give, therefore, in Table 3.4.4.4 only possible symmetries T_{1j} and $\overline{\mathsf{J}}_{1j}$ of non-ferroelastic domain twins and walls, together with their classification, without specifying the orientation of the wall plane p.

Non-ferroelastic domain walls are usually curved with a slight preference for certain orientations (see Figs. 3.4.1.5 and 3.4.3.3). Such shapes indicate a weak anisotropy of the wall energy σ, *i.e.* small changes of σ with the orientation of the wall. The situation is different in ferroelectric domain structures, where charged domain walls have higher energies than uncharged ones.

A small energetic anisotropy of non-ferroelastic domain walls is utilized in producing *tailored domain structures* (Newnham *et al.*, 1975). A required domain pattern in a non-ferroelastic ferroelectric crystal can be obtained by evaporating electrodes of a desired shape (*e.g.* stripes) onto a single-domain plate cut perpendicular to the spontaneous polarization $\mathbf{P}_0$. Subsequent poling by an electric field switches only regions below the electrodes and thus produces the desired antiparallel domain structure.

Periodically poled ferroelectric domain structures fabricated by this technique are used for example in quasi-phase-matching optical multipliers (see *e.g.* Shur *et al.*, 1999, 2001; Rosenman *et al.*, 1998). An example of such an *engineered domain structure* is presented in Fig. 3.4.4.3.

Anisotropic domain walls can also appear if the Landau free energy contains a so-called Lifshitz invariant (see Section 3.1.3.3), which lowers the energy of walls with certain orientations and can be responsible for the appearance of an incommensurate phase (see *e.g.* Dolino, 1985; Tolédano & Tolédano, 1987; Tolédano & Dmitriev, 1996; Strukov & Levanyuk, 1998). The irreversible character of domain walls in a commensurate phase of crystals also containing (at least theoretically) an incommensurate phase has been confirmed in the frame of phenomenological theory by Ishibashi (1992). The incommensurate structure in quartz that demonstrates such an anisotropy is discussed at the end of the next example.

Table 3.4.4.4. *Symmetries of non-ferroelastic domain twins and walls*

T_{1j}	$\overline{\mathsf{J}}_{1j}$	Classification
1	1	AI
1	$\bar{1}$	AR
	$\underline{2}$	AR
	$2^\star$	AR*
	$m^\star$	AR*
$\bar{1}^\star$	$\bar{1}^\star$	SI
	$\underline{2}/m^\star$	SR
	$2^\star/\underline{m}$	SR
2	$2m^\star m^\star$	AR*
$\underline{2}^\star$	$\underline{2}^\star$	SI
	$\underline{2}^\star/m^\star$	SR
	$2^\star\underline{2}^\star\underline{2}$	SR
	$\underline{2}^\star\underline{m}m^\star$	SR
m	m	AI
	$\underline{2}/m$	AR
	$2^\star mm^\star$	AR*
$\underline{m}^\star$	$\underline{m}^\star$	SI
	$2^\star/\underline{m}^\star$	SR
	$\underline{m}^\star m^\star\underline{2}$	SR
$\underline{2}^\star/m$	$\underline{2}^\star/m$	SI
	$m\underline{m}m^\star$	SR
$2/\underline{m}^\star$	$2/\underline{m}^\star$	SI
	$m^\star m^\star\underline{m}^\star$	SR
	$4^\star/\underline{m}^\star$	SR
$2\underline{2}^\star\underline{2}^\star$	$2\underline{2}^\star\underline{2}^\star$	SI
	$\underline{m}m^\star m^\star$	SR
	$4^\star\underline{2}\underline{2}^\star$	SR
	$\bar{4}\underline{2}^\star m^\star$	SR
$\underline{m}^\star m\underline{2}^\star$	$\underline{m}^\star m\underline{2}^\star$	SI
	$\underline{m}^\star mm^\star$	SR
$mm\underline{m}^\star$	$mm\underline{m}^\star$	SI
	$4^\star/\underline{m}^\star m^\star m$	SR
4	$4m^\star m^\star$	AR*
$\bar{4}^\star$	$\bar{4}^\star 2m^\star$	SR
$4/\underline{m}^\star$	$4/\underline{m}^\star$	SI
	$4/\underline{m}^\star m^\star m^\star$	SR
$4\underline{2}^\star\underline{2}^\star$	$4\underline{2}^\star\underline{2}^\star$	SI
	$4/\underline{m}m^\star m^\star$	SR
$\bar{4}^\star 2^\star m$	$4^\star/\underline{m}m^\star m$	SR
$4/\underline{m}^\star mm$	$4/\underline{m}^\star mm$	SI
3	$3m^\star$	AR*
	$6^\star$	AR*
$\bar{3}^\star$	$\bar{3}^\star$	SI
	$\bar{3}^\star m^\star$	SR
	$6^\star/\underline{m}$	SR
$3m$	$6^\star mm^\star$	AR*
$3\underline{2}^\star$	$3\underline{2}^\star$	SI
	$\bar{3}m^\star$	SR
	$6^\star\underline{2}\underline{2}^\star$	SR
	$\bar{6}\underline{2}^\star m^\star$	SR
$\bar{3}^\star m$	$\bar{3}^\star m$	SI
	$6^\star/\underline{m}mm^\star$	SR
6	$6m^\star m^\star$	AR*
$\bar{6}^\star$	$\bar{6}^\star$	SI
	$6^\star/\underline{m}^\star$	SR
	$\bar{6}^\star\underline{2}m^\star$	SR
$6/\underline{m}^\star$	$6/\underline{m}^\star$	SI
	$6/\underline{m}^\star m^\star m^\star$	SR
$6\underline{2}^\star\underline{2}^\star$	$6\underline{2}^\star\underline{2}^\star$	SI
	$6/\underline{m}m^\star m^\star$	SR
$\bar{6}^\star m\underline{2}^\star$	$\bar{6}^\star m\underline{2}^\star$	SI
	$6^\star/\underline{m}^\star mm^\star$	SR
$6/\underline{m}^\star mm$	$6/\underline{m}^\star mm$	SI

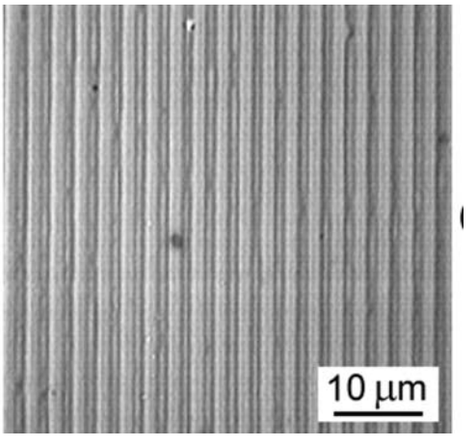

Fig. 3.4.4.3. Engineered periodic non-ferroelastic ferroelectric stripe domain structure within a lithium tantalate crystal with symmetry descent $\bar{6} \supset 3$. The domain structure is revealed by etching and observed in an optical microscope (Shur *et al.*, 2001). Courtesy of Vl. Shur, Ural State University, Ekaterinburg.

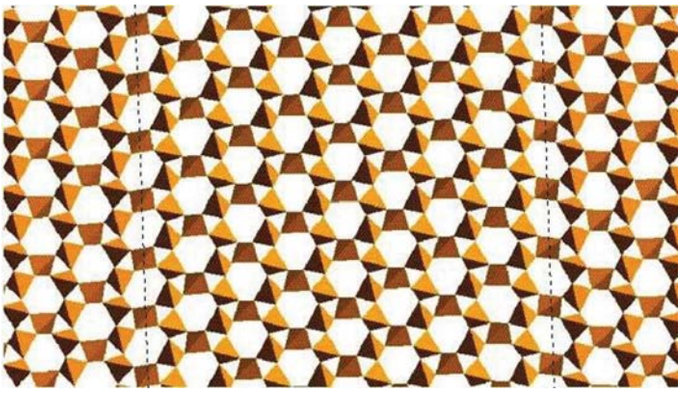

Fig. 3.4.4.4. Microscopic structure of two domain states and two parallel mutually reversed domain walls in the α phase of quartz. The left-hand vertical dotted line represents the domain wall W_{12}, the right-hand line is the reversed domain wall W_{12}. To the left of the left-hand line and to the right of the right-hand line are domains with domain state $\mathbf{S}_1$, the domain between the lines has domain state $\mathbf{S}_2$. For more details see text. Courtesy of M. Calleja, University of Cambridge.

Example 3.4.4.2. Domain walls in the α phase of quartz. Quartz (SiO_2) undergoes a structural phase transition from the parent β phase (symmetry group $6_z2_x2_y$) to the ferroic α phase (symmetry 3_z2_x). The α phase can appear in two domain states $\mathbf{S}_1$ and $\mathbf{S}_2$, which have the same symmetry $F_1 = F_2 = 3_z2_x$. The symmetry J_{12} of the unordered domain pair $\{\mathbf{S}_1, \mathbf{S}_2\}$ is given by $J_{12}^\star = 3_z2_x \cup 2_y^*\{3_z2_x\} = 6_z^*2_x2_y^*$.

Table 3.4.4.5 summarizes the results of the symmetry analysis of domain walls (twins). Each row of the table contains data for one representative domain wall $\mathbf{W}_{12}(\mathbf{n}_{12})$ from one orbit $G\mathbf{W}_{12}(\mathbf{n}_{12})$. The first column of the table specifies the normal $\mathbf{n}$ of the wall plane p, further columns list the layer groups $\widehat{\mathsf{F}}_{12}$, T_{12} and $\overline{\mathsf{J}}_{12}$ that describe the symmetry properties and classification of the wall (defined in Table 3.4.4.3), and n_W is the number of symmetry-equivalent domain walls [*cf.* equation (3.4.4.21)].

The last two columns give possible components of the spontaneous polarization $\mathbf{P}$ of the wall $\mathbf{W}_{12}(\mathbf{n})$ and the reversed wall $\mathbf{W}_{21}(\mathbf{n})$. Except for walls with normals [001] and [100], all walls are polar, *i.e.* they can be spontaneously polarized. The reversal of the polarization in reversible domain walls requires the reversal of domain states. In irreversible domain walls, the reversal of $\mathbf{W}_{12}$ into $\mathbf{W}_{21}$ is accompanied by a change of the polarization $\mathbf{P}$ into $\mathbf{P}'$, which may have a different absolute value and direction different to that of $\mathbf{P}$.

The structure of two domain states and two mutually reversed domain walls obtained by molecular dynamics calculations are depicted in Fig. 3.4.4.4 (Calleja *et al.*, 2001). This shows a projection on the *ab* plane of the structure represented by SiO_4 tetrahedra, in which each tetrahedron shares four corners. The threefold symmetry axes in the centres of distorted hexagonal channels and three twofold symmetry axes (one with vertical orientation) perpendicular to the threefold axes can be easily seen. The two vertical dotted lines are the wall planes p of two mutually reversed walls $[\mathbf{S}_1[010]\mathbf{S}_2] = \mathbf{W}_{12}[010]$ and $[\mathbf{S}_2[010]\mathbf{S}_1] = \mathbf{W}_{21}[010]$. In Table 3.4.4.5 we find that these walls have the symmetry $\mathsf{T}_{12}[010] = \mathsf{T}_{21}[010] = \underline{2}_x2_y^\star\underline{2}_z^\star$, and in Fig. 3.4.4.4 we can verify that the operation $\underline{2}_x$ is a 'side-reversing' operation $\underline{s}_{12}$ of the wall (and the whole twin as wall), operation $2_y^\star$ is a 'state-exchanging operation' $r_{12}^\star$ and the operation $\underline{2}_z^\star$ is a non-trivial 'side-and-state reversing' operation $\underline{t}_{12}^\star$ of the wall. The walls $\mathbf{W}_{12}[010]$ and $\mathbf{W}_{21}[010]$ are, therefore, symmetric and reversible walls.

During a small temperature interval above the appearance of the α phase at 846 K, there exists an incommensurate phase that can be treated as a regular domain structure, consisting of triangular columnar domains with domain walls (discommensurations) of negative wall energy σ (see *e.g.* Dolino, 1985). Both theoretical considerations and electron microscopy observations (see *e.g.* Van Landuyt *et al.*, 1985) show that the wall normal has the $[uv0]$ direction. From Table 3.4.4.5 it follows that there are six equivalent walls that are symmetric but irreversible, therefore any two equivalent walls differ in orientation.

This prediction is confirmed by electron microscopy in Fig. 3.4.4.5, where black and white triangles correspond to domains with domain states $\mathbf{S}_1$ and $\mathbf{S}_2$, and the transition regions between black and white areas to domain walls (discommensurations). To a domain wall of a certain orientation no reversible wall appears with the same orientation but with a reversed order of black and white. Domain walls in homogeneous triangular parts of the structure are related by 120 and 240° rotations and carry, therefore, parallel spontaneous polarizations; wall orientations in two differently oriented blocks (the middle of the right-hand part and the rest on the left-hand side) are related by 180° rotations about the axis 2_x in the plane of the photograph and are, therefore, polarized in antiparallel directions (for more details see Saint-Grégoire & Janovec, 1989; Snoeck *et al.*, 1994). After cooling down to room temperature, the wall energy becomes positive and the regular domain texture changes into a coarse domain struc-

Table 3.4.4.5. *Symmetry properties of domain walls in α quartz*

$|\mathbf{P}| \neq |\mathbf{P}'|,\ P_i' \neq -P_i,\ i = x, y, z.$

n	$\widehat{\mathsf{F}}_{12}$	T_{12}	$\overline{\mathsf{J}}_{12}$	Classification	n_W	$\mathbf{P}(\mathbf{W}_{12})$	$\mathbf{P}(\mathbf{W}_{21})$
[001]	3_z	$3_z\underline{2}_y^*$	$6_z^*\underline{2}_x\underline{2}_y^*$	SR	2		
[100]	2_x	$2_x\underline{2}_y^*2_z^*$	$2_x\underline{2}_y^*\underline{2}_z^*$	SI	3		
[010]	1	$\underline{2}_z^*$	$\underline{2}_x2_y^*\underline{2}_z^*$	SR	6	$0, 0, P_z$	$0, 0, -P_z$
$[0vw]$	1	1	$\underline{2}_x$	A$\underline{\mathsf{R}}$	12	P_x, P_y, P_z	$P_x, -P_y, -P_z$
$[u0w]$	1	$\underline{2}_y^*$	$\underline{2}_y^*$	SI	6	$0, P_y, 0$	$0, -P_y', 0$
$[uv0]$	1	$\underline{2}_z^*$	$\underline{2}_z^*$	SI	6	$0, 0, P_z$	$0, 0, P_z'$
$[uvw]$	1	1	1	AI	12	P_x, P_y, P_z	P_x', P_y', P_z'

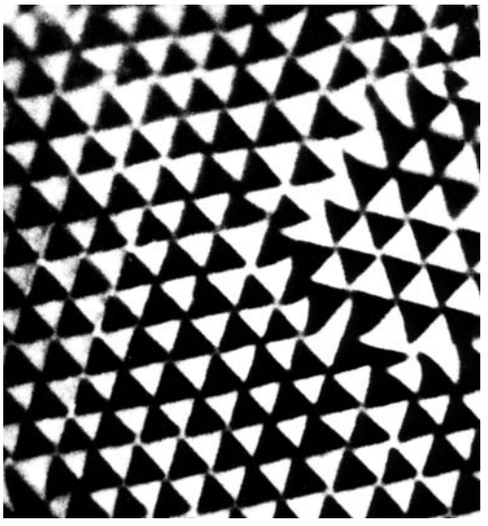

Fig. 3.4.4.5. Transmission electron microscopy (TEM) image of the incommensurate triangular ($3-q$ modulated) phase of quartz. The black and white triangles correspond to domains with domain states $\mathbf{S}_1$ and $\mathbf{S}_2$, and the transition regions between black and white areas to domain walls (discommensurations). For a domain wall of a certain orientation there are no reversed domain walls with the same orientation but reversed order of black and white; the walls are, therefore, non-reversible. Domain walls in regions with regular triangular structures are related by 120 and 240° rotations about the z direction and carry parallel spontaneous polarizations (see text). Triangular structures in two regions (blocks) with different orientations of the triangles are related *e.g.* by 2_x and carry, therefore, antiparallel spontaneous polarizations and behave macroscopically as two ferroelectric domains with antiparallel spontaneous polarization. Courtesy of E. Snoeck, CEMES, Toulouse and P. Saint-Grégoire, Université de Toulon.

ture in which these six symmetry-related wall orientations still prevail (Van Landuyt *et al.*, 1985).

3.4.4.5. *Ferroelastic domain twins and walls. Ferroelastic twin laws*

As explained in Section 3.4.3.6, from a domain pair $(\mathbf{S}_1, \mathbf{S}_j)$ of ferroelastic single-domain states with two perpendicular equally deformed planes p and p' one can form four different ferroelastic twins (see Fig. 3.4.3.8). Two mutually reversed twins $(\mathbf{S}_1|\mathbf{n}|\mathbf{S}_j)$ and $(\mathbf{S}_j|\mathbf{n}|\mathbf{S}_1)$ have the same twin symmetry $\mathsf{T}_{1j}(p)$ and the same symmetry $\overline{\mathsf{J}}_{1j}(p)$ of the twin pair $(\mathbf{S}_1, \mathbf{S}_j|\mathbf{n}|\mathbf{S}_j, \mathbf{S}_1)$. The *ferroelastic twin laws* can be expressed by the layer group $\overline{\mathsf{J}}_{1j}(p)$ or, in a less complete way (without specification of reversibility), by the twin symmetry $\mathsf{T}_{1j}(p)$. The same holds for two mutually reversed twins $(\mathbf{S}_1|\mathbf{n}'|\mathbf{S}_j)$ and $(\mathbf{S}_j|\mathbf{n}'|\mathbf{S}_1)$ with a twin plane p' perpendicular to p.

Table 3.4.4.6 summarizes possible symmetries T_{1j} of ferroelastic domain twins and corresponding ferroelastic twin laws $\overline{\mathsf{J}}_{1j}$. Letters V and W signify strain-dependent and strain-independent (with a fixed orientation) domain walls, respectively. The classification of domain walls and twins is defined in Table 3.4.4.3. The last column contains twinning groups $K_{1j}(F_1)$ of ordered domain pairs $(\mathbf{S}_1, \mathbf{S}_j)$ from which these twins can be formed. The symbol of K_{1j} is followed by a symbol of the group F_1 given in square brackets. The twinning group $K_{1j}(F_1)$ specifies, up to two cases, a class of equivalent domain pairs [orbit $G(\mathbf{S}_1, \mathbf{S}_j)$] (see Section 3.4.3.4). More details on particular cases (orientation of domain walls, disorientation angle, twin axis) can be found in synoptic Table 3.4.3.6. From this table follow two general conclusions:

(1) All layer groups describing the symmetry of compatible ferroelastic domain walls are polar groups, therefore *all compatible ferroelastic domain walls in dielectric crystals can be spontaneously polarized*. The direction of the spontaneous polarization is parallel to the intersection of the wall plane p and the plane of shear (*i.e.* a plane perpendicular to the axis of the ferroelastic domain pair, see Fig. 3.4.3.5*b* and Section 3.4.3.6.2).

(2) *Domain twin* $(\mathbf{S}_1|\mathbf{n}|\mathbf{S}_j)$ *formed in the parent clamping approximation from a single-domain pair* $(\mathbf{S}_1, \mathbf{S}_j)$ *and the relaxed domain twin* $(\mathbf{S}_1^+|\mathbf{n}|\mathbf{S}_j^-)$ *with disoriented domain states have the same symmetry groups* T_{1j} and $\overline{\mathsf{J}}_{1j}$.

This follows from simple reasoning: all twin symmetries T_{1j} in Table 3.4.4.6 have been derived in the parent clamping approximation and are expressed by the orthorhombic group *mm*2 or by some of its subgroups. As shown in Section 3.4.3.6.2, the maximal symmetry of a mechanically twinned crystal is also *mm*2. An additional simple shear accompanying the lifting of the parent clamping approximation cannot, therefore, decrease the symmetry $\mathsf{T}_{1j}(p)$ derived in the parent clamping approximation. In a similar way, one can prove the statement for the group $\overline{\mathsf{J}}_{1j}(p)$ of the twin pairs $(\mathbf{S}_1, \mathbf{S}_j|\mathbf{n}|\mathbf{S}_j, \mathbf{S}_1)$ and $(\mathbf{S}_1^+, \mathbf{S}_j^-|\mathbf{n}|\mathbf{S}_j^-, \mathbf{S}_1^+)$.

3.4.4.6. *Domain walls of finite thickness – continuous description*

A domain wall of zero thickness is a geometrical construct that enabled us to form a twin from a domain pair and to find a layer group that specifies the *maximal symmetry* of that twin. However, real domain walls have a finite, though small, thickness. Spatial changes of the structure within a wall may, or may not, lower the wall symmetry and can be conveniently described by a *phenomenological theory*.

We shall consider the simplest case of a one nonzero component η of the order parameter (see Section 3.1.2). Two nonzero equilibrium homogeneous values of $-\eta_0$ and $+\eta_0$ of this parameter correspond to two domain states $\mathbf{S}_1$ and $\mathbf{S}_2$. Spatial changes of the order parameter in a domain twin $(\mathbf{S}_1|\mathbf{n}|\mathbf{S}_2)$ with a zero-thickness domain wall are described by a step-like function $\eta(\xi) = -\eta_0$ for $\xi < 0$ and $\eta(\xi) = +\eta_0$ for $\xi > 0$, where ξ is the distance from the wall of zero thickness placed at $\xi = 0$.

A domain wall of finite thickness is described by a function $\eta(\xi)$ with limiting values $-\eta_0$ and η_0:

$$\lim_{\xi\to-\infty} \eta(\xi) = -\eta_0, \quad \lim_{\xi\to+\infty} \eta(\xi) = \eta_0. \tag{3.4.4.23}$$

If the wall is symmetric, then the profile $\eta(\xi)$ in one half-space, say $\xi < 0$, determines the profile in the other half-space $\xi > 0$. For continuous $\eta(\xi)$ fulfilling conditions (3.4.4.23) this leads to the condition

$$\eta(\xi) = -\eta(-\xi), \tag{3.4.4.24}$$

i.e. $\eta(\xi)$ must be an odd function. This requirement is fulfilled if there exists a non-trivial symmetry operation of a domain wall (twin): a side reversal ($\xi \to -\xi$) combined with an exchange of domain states [$\eta(\xi) \to -\eta(\xi)$] results in an identical wall profile.

A particular form of the wall profile $\eta(\xi)$ can be deduced from Landau theory. In the simplest case, the dependence $\eta(\xi)$ of the domain wall would minimize the free energy

$$\int_{-\infty}^{\infty} \left(\Phi_0 + \tfrac{1}{2}\alpha(T - T_c)\eta^2 + \tfrac{1}{4}\beta\eta^4 + \tfrac{1}{2}\delta\left(\frac{d^2\eta}{d\xi^2}\right)^2 \right) \mathrm{d}\xi, \tag{3.4.4.25}$$

where α, β, δ are phenomenological coefficients and T and T_c are the temperature and the temperature of the phase transition, respectively. The first three terms correspond to the homogeneous part of the Landau free energy (see Section 3.2.1) and the last term expresses the energy of the spatially changing order parameter. This variational task with boundary conditions (3.4.4.23) has the following solution (see *e.g.* Salje, 1990, 2000*b*; Ishibashi, 1990; Strukov & Levanyuk, 1998)

$$\eta(\xi) = \eta_0 \tanh(\xi/w), \tag{3.4.4.26}$$

where the value w specifies one half of the *effective thickness* $2w$ *of the domain wall* and is given by